Mechanism of Base-Catalyzed Schiff Base Deprotonation in Halorhodopsin†

Janos K. Lanyi
Department of Physiology and Biophysics, University of California, Irvine, California 92717
Received April 17, 1986; Revised Manuscript Received June 26, 1986

ABSTRACT: It has been shown earlier that the deprotonation of the Schiff base of illuminated halorhodopsin proceeds with a much lower pK_a than that of the unilluminated pigment and the reversible protonation change is catalyzed by azide and cyanate [Hegemann, P., Oesterhelt, D., & Steiner, M. (1985) *EMBO J. 4*, 2347–2350]. We have studied the kinetics of the proton-transfer events with flash spectroscopy and compared a variety of anionic bases with different pK_a with regard to their apparent binding constants and their catalytic activities. The results suggest a general base catalysis mechanism in which the anionic bases bind with apparently low affinity to halorhodopsin, although with some degree of size- and/or shape-dependent specificity. The locus of the catalysis is accessible from the cytoplasmic side of the membrane and is not at site I, where various anions bind and shift the pK_a of the deprotonation. Neither is it at site II, where a few specific anions (like chloride) bind to the all-trans pigment. It may be concluded that while the all-trans pigment loses its Schiff base proton very rapidly at its pK_a, there is a kinetic barrier to this deprotonation in the 13-cis photointermediate that can be partially overcome by the reversible protonation of an extrinsic anionic base, which shuttles protons between the interior of the protein and the aqueous medium. The need for an extrinsic proton acceptor for efficient deprotonation of the Schiff base of halorhodopsin is one of the main differences between this pigment and the analogous retinal protein, bacteriorhodopsin.

Halorhodopsin is a retinal protein, found in the cytoplasmic membrane of halobacteria, which is similar in some respects to bacteriorhodopsin but functions as a light-driven inward-directed chloride pump (Schobert & Lanyi, 1982; Bamberg et al., 1984), rather than as an outward-directed proton pump. As in bacteriorhodopsin, interaction between the retinal and the protein causes the absorption maximum of halorhodopsin to be red-shifted to 570–580 nm, as compared to the absorption maximum of free retinal at 380 nm. Two binding sites for anions have been described, which further affect the spectroscopic properties of halorhodopsin: site I, a relatively nonspecific site on the surface of the protein, whose occupancy causes a small blue-shift and an increase in the pK_a of the deprotonation of the retinal Schiff base (Schobert et al., 1986; Schobert & Lanyi, 1986), and site II, a site specific for the transported anions (chloride, bromide, and iodide), whose occupancy causes a small red-shift (Ogurusu et al., 1982; Ogurusu et al., 1984; Steiner et al., 1984; Schobert et al., 1986) but no change in the pK_a (Schobert et al., 1986). Flash spectroscopy has revealed that after absorption of a photon the pigment undergoes a cyclic reaction on a millisecond time scale (photocycle) with several spectroscopicaly distinct intermediates (Stoeckenius & Bogomolni, 1982; Schobert et al., 1983; Lanyi & Vodyanoy, 1986). Kinetic analyses of steady-state (Oesterhelt et al., 1985) and single turnover (Lanyi & Vodyanoy, 1986) data obtained with purified, detergent-solubilized halorhodopsin have suggested a photocycle scheme in the presence of chloride, in which the short-lived photoproduct[1] HR_{600}·Cl (Polland et al., 1985) decays into HR_{520}·Cl^-, which is in a chloride-dependent equilibrium with HR_{640} (Oesterhelt et al., 1985). The latter decays into HR_{565} in a chloride-independent manner and upon chloride binding is converted into the parent species, HR_{578}·Cl^-. In the absence of chloride HR_{565} undergoes a simpler photocycle, with only HR_{640} as long-lived intermediate (Lanyi & Vodyanoy, 1986). Thus, there are two chloride-dependent equilibria in the photocycle: between the species that exist in the dark, HR_{565} and HR_{578}·Cl^- (chloride binding at site II), and between the photointermediates HR_{640} and HR_{520}·Cl^-. The affinity of HR_{565} to chloride is far higher than that of HR_{640}, probably related to the fact that in the former the retinal is all-trans (Smith et al., 1984; Maeda et al., 1985; Alshuth et al., 1985) while in the latter it is cis, most probably 13-cis (Lanyi, 1984a; Lanyi & Vodyanoy, 1986). The photocycle is thus accompanied by the cyclic release and uptake of chloride. Binding of chloride to site II is on the side of the membrane from which chloride is transported. If the release of chloride from HR_{520}·Cl^- were to be on the other side of the membrane, a possibility under investigation in this laboratory, the cyclic debinding and rebinding during the photocycle would result in vectorial chloride movement across the membrane, as expected for a chloride pump.

The key events in the photocycle of bacteriorhodopsin are the deprotonation and reprotonation of the retinal Schiff base (Lewis et al., 1974), and it has been proposed that this proton is lost and regained in a vectorial fashion, resulting in the net proton translocation that constitutes transport (for reviews see: Stoeckenius et al., 1979; Stoeckenius & Bogomolni, 1982; Lanyi, 1984b). During the photocycle a proton may be exchanged between the Schiff base and two reversibly protonated aspartate residues (Engelhard et al., 1985). The photocycle of halorhodopsin does not contain such an obligatory deprotonation step, but under some conditions reversible deprotonation of the Schiff base can be observed in this system also (Lanyi & Schobert, 1983; Steiner et al., 1984; Hegemann et al., 1985a). For example, it has been shown that the all-trans pigment in the dark is in rapid equilibrium with its depro-

† This work was supported by grants from the Department of Energy (DE-AT03-ER10637) and the National Institutes of Health (NIH GM 29498).

[1] Abbreviations: halorhodopsin species are represented by $HR_{wavelength}$, with chloride binding to site II indicated as ·Cl^-, and superscript D or L following the designation indicates origin in the dark or in the light; MES, 2-(*N*-morpholino)ethanesulfonic acid; EPPS, *N*-(2-hydroxyethyl)-piperazine-*N*′-3-propanesulfonic acid; TPP^+, tetraphenylphosphonium ion.

0006-2960/86/0425-6706$01.50/0

tonated form, which absorbs at 410 nm and is termed HR_{410}^{D}, with a pK_a of 7.4 in the absence of site I anions and 8.9 in their presence (Schobert et al., 1986). The 13-cis pigment, which appears during the photocycle, deprotonates with a lower pK_a, estimated to be 4.8 in 1 M NaCl (Oesterhelt et al., 1985), but the proton loss, as well as the reprotonation, is much slower than the recovery of the parent halorhodopsin. Hence, at a pH below the pK_a of the deprotonation in the dark, a deprotonated halorhodopsin, HR_{410}^{L}, will accumulate, but only during prolonged illumination. Azide and cyanate were found to increase the rate of deprotonation to an extent that allowed effective competition with the completion of the normal photocycle, so that HR_{410}^{L} could accumulate readily (Hegemann et al., 1985a). Because reprotonation was equally accelerated and thus the steady-state ratio of deprotonated and protonated halorhodopsin was independent of the concentration of the azide (Hegemann et al., 1985a), the process was described as catalysis, i.e., general base catalysis. Blue light was found to drive the transport-inactive HR_{410}^{L} back to the transport-active protonated form, while yellow light reversed this transformation (Hegemann et al., 1985b), leading to a suggestion that this photochromic process might have a physiologically relevant regulatory function.

We describe here further studies of the de- and reprotonation of the halorhodopsin Schiff base, using flash-spectroscopy to determine the individual rate constants of the two base-catalyzed processes. The questions addressed here include the natures of the proton-transfer reactions and the interaction between protein and proton acceptor. The results reveal differences in the environment of the Schiff base in the different halorhodopsin species and suggest that halorhodopsin and bacteriorhodopsin differ in the accessibility of the protein interior to protons from the medium.

Materials and Methods

Growth of halobacteria and preparation of purified halorhodopsin were as previously described (Steiner & Oesterhelt, 1983), except that the detergent Lubrol was not replaced with octylglucoside. The pigment was stored at 4 °C in the dark in 4 M NaCl, 20 mM MES, pH 6.0, and 1–4% Lubrol PX and was dialyzed against the desired buffer before use, as before. For experiments in a chloride-free medium, the buffer used was 0.5 M Na_2SO_4, 0.2 M $NaNO_3$, and 50 mM MES, pH 6.0. Where azide or other catalysts were added, the pH of the stock solutions (0.5–2 M) was adjusted to 6.0. Cell envelope vesicles were prepared as previously described (Lanyi & MacDonald, 1979) and stored in unbuffered 4 or 5 M NaCl at 4 °C.

Flash spectrophotometry was in the cross-beam instrument described before (Schobert et al., 1983; Lanyi & Vodyanoy, 1986). In all experiments, traces from 512 flashes were averaged. Because the decay of HR_{410}^{L} was slow, the accumulation of this photoproduct during the flash regime (and the consequent negative base line in the absorbance traces corresponding to its reprotonation) had to be avoided by appropriate selection of low flash frequency and intensity, even when this resulted in lower signal/noise ratio than in previous studies. The traces were recorded on floppy disks for the subsequent analysis, in which the traces were compared with the predictions of a kinetic model with adjustable rate constants, as before (Lanyi & Vodyanoy, 1986).

Light-dependent absorption changes at 400 nm were followed by placing detergent-solubilized halorhodopsin (as in the flash experiments) in a 10-mm path length thermostated cuvette (at 15 °C) and measuring absorption as a function of time in a Shimadzu Model 250 spectrophotometer while the sample was illuminated at a 90° angle with green light. The photomultiplier was protected with a 400-nm interference filter. The sample was illuminated with blue light to regenerate the pigment after each experiment; absorption spectra were taken to ascertain full reprotonation.

Light-driven transport was assayed by following the appearance of membrane potential (negative inside) in cell envelope vesicles with a tetraphenylphosphonium (TPP^+) electrode, built according to Kamo et al. (1982). The total volume was 7 mL in a stirred chamber, thermostated at 22 °C and illuminated with two 250-W tungsten–halogen lamps through 2 cm of water and 530-nm long-pass filters. The assay mixture contained 4 M NaCl and 100 mM EPPS, pH 8.0. Vesicle concentration was 2 mg/mL protein, and TPP^+ concentration was 5 μM. When the interior of the vesicles was to be buffered, the vesicles equilibrated with 5 M NaCl were diluted 15-fold (osmotically shocked) with 4 M NaCl *plus* EPPS buffer and assayed after 10-min incubation. In the controls, where the interior was to remain unbuffered, the vesicles were diluted with 4 M NaCl solution and incubated 10 min and the EPPS buffer was then added as a concentrated stock solution.

Results

Kinetic Analysis of the Azide-Catalyzed Reversible Deprotonation of the Halorhodopsin Schiff Base. The formation and decay of HR_{410}^{L} was followed by flash spectroscopy of purified halorhodopsin without azide and in the presence of various amounts of added azide. The buffer used contained 0.5 M Na_2SO_4 (sulfate being an anion that does not bind to the pigment but provides high ionic strength) plus 0.2 M $NaNO_3$ (a site I anion that provided protection from photodestruction by the flashes). Representative traces of absorbance changes at 410 nm are shown in Figure 1. These traces were analyzed with an extended version of the kinetic model described earlier for the halorhodopsin photocycle (Lanyi & Vodyanoy, 1986). The modified photocycle, which includes the deprotonation of the HR_{640} photointermediate, is shown in Figure 2, where in the absence of chloride only the formation and decay of HR_{640} and its de- and reprotonation need to be considered. The differential equations that describe this process are

$$\frac{d[HR_{640}]}{dt} = k_5[HR_{410}][H^+] - [k_3 + k_4][HR_{640}] \quad (1)$$

$$\frac{d[HR_{410}]}{dt} = k_4[HR_{640}] - k_5[HR_{410}][H^+] \quad (2)$$

The rate constant for the $HR_{640} \rightarrow HR_{565}$ reaction, k_3 in Figure 2, could be determined by measuring the absorption change at 660 nm in the absence of azide (Lanyi & Vodyanoy, 1986). As before, the amount of HR_{640} formed during the flash depended on the concentration of the pigment and the amount of light absorbed by the sample. This parameter was introduced into the model by matching the absorbance change immediately after the flash with that in the computer-generated traces based on eq 1 and 2. Under these conditions no appreciable amount of HR_{410}^{L} was formed (Figure 1A) and k_4 and k_5 were set to zero. Matching the decay in the simulated trace to that in the experimental trace then allowed the estimation of k_3. Next, azide was added at increasing concentrations, and the traces obtained at 410 nm (Figures 1B–D, solid lines) were compared with the predictions of the model (Figures 1B–D, dashed lines), using various k_4 and k_5 values until good fits were obtained. Choosing the best k_5 values was by fitting the decay phase in the traces. Choosing the best k_4 values was based on the fact that the amplitude of the

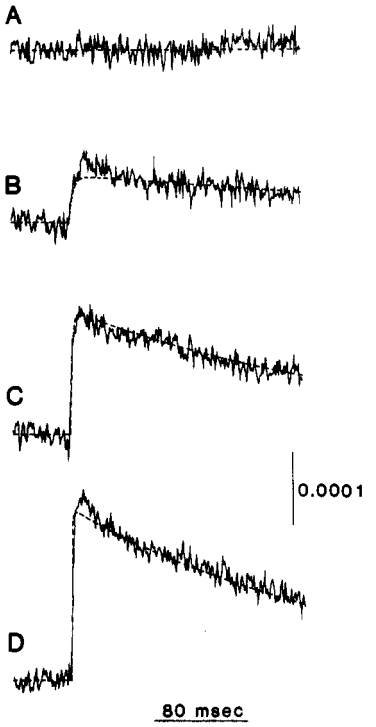

FIGURE 1: Azide-catalyzed formation and decay of HR_{410}^{L} in the absence of chloride. Halorhodopsin (2.8 nmol/mL) was in 0.5 M Na_2SO_4, 0.2 M $NaNO_3$, and 50 mM MES, pH 6.0. Flash-induced absorbance change at 410 nm is shown, with the absorbance change/flash indicated on the vertical scale, and the time sweep on the horizontal scale. Azide concentration: (A) zero; (B) 10 mM; (C) 30 mM; (D) 70 mM. Solid line, experimental traces; dashed line, simulated traces. The small transient upward deflections in some of the traces are artifacts.

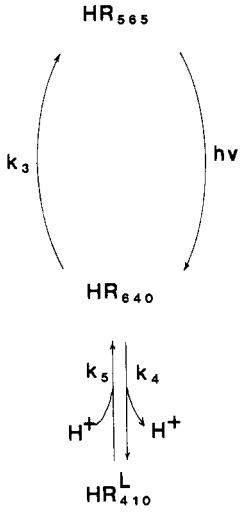

FIGURE 2: Extended kinetic model for the halorhodopsin photocycle in the absence of chloride, with the deprotonation of the photointermediate HR_{640} included. Detailed description of the complete photocycle is found in Oesterhelt et al. (1985) and Lanyi et al. (1986), where k_1 and k_2 are also defined. The primary photoproduct is not shown. The reaction not labeled with a rate constant is considered instantaneous on a millisecond time scale.

absorption change depended mainly on this parameter.

Figure 3 shows k_4 and k_5, determined as described above, at increasing azide concentrations. The dependency on azide appears to be linear up to at least 100 mM. The rate constants in Figure 3 are both approximately 10-fold greater than those earlier calculated at a given azide concentration from macroscopic rates in steady-state and flash experiments, e.g., from the rate of HR_{410}^{L} decay after continuous illumination and

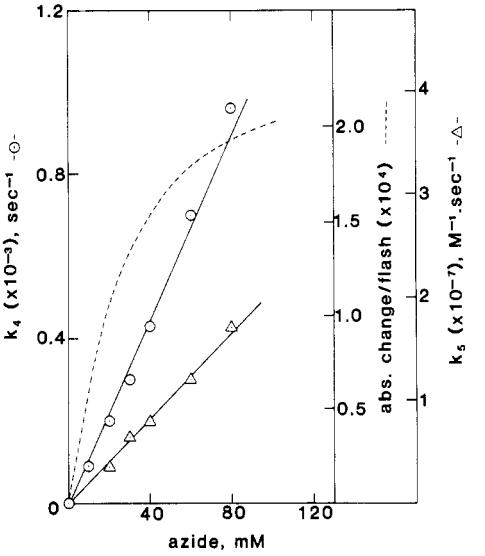

FIGURE 3: Dependency of deprotonation and reprotonation rate constants on azide concentration. Rates are estimated with the kinetic model, as described in the text and shown in Figure 1: k_4, (⊙); k_5, (△); dashed line, predicted amplitude of maximal absorbance change after the flash.

from rate of absorption increase in flash traces (Oesterhelt et al., 1985). The discrepancy might originate from the different detergents used, but k_3 and k_1/k_2 in the two reports agree within a factor of 2. Also plotted in Figure 3 is the maximal absorbance change after the flash (dashed line), predicted by the chosen values of k_3, k_4, and k_5. This parameter shows apparent saturation with increasing azide concentration.

The signal/noise ratio of the flash method did not allow careful examination of the deprotonation process at very low azide concentrations, but absorption changes during sustained illumination could be measured under these conditions with good accuracy, as in Hegemann et al., (1985a). Although not shown, such experiments have revealed that the initial rate of the deprotonation is strictly linearly dependent on azide concentration between 0 and 1 mM azide, as at the higher concentrations. Thus, no cooperativity could be demonstrated in the kinetics of the deprotonation, and there is no reason to suppose that more than one azide is necessary for the proton transfer.

Comparison of the Catalytic Activity of Various Bases. In principle all bases with suitable pK_a should act as proton acceptors and donors in a reversible deprotonation. In comparing various bases, we made use of the following line of reasoning. Since the rate constants k_4 and k_5 were linearly dependent on azide concentration (Figure 3), as well as on the concentration of all the other bases tested (not shown), the deprotonation and reprotonation reactions could be suitably analyzed by postulating the following bimolecular reaction mechanism for the two processes, at least in the concentration ranges tested:

$$HR_{640} + B^- \leftrightarrow HR_{410}^{L} + HB \quad (3)$$

$$HB \leftrightarrow H^+ + B^- \quad (4)$$

That is to say, the base B^- acts as proton acceptor and its conjugate acid acts as proton donor. Formally, this model gives rise to the same equations as (1) and (2), with

$$k_{deprot} = k_4/[B^-] = k_4/[base] \quad (5)$$

$$k_{prot} = k_5 \times 10^{-pK_a}/[base] \quad (6)$$

where k_{deprot} and k_{prot} are the rate constants of the forward

Table I: Kinetic Parameters for the Catalysis of Protonation Reactions of the Schiff Base in HR_{640}[a]

base	pK_a	k_{deprot} ($M^{-1}\cdot s^{-1}$)	k_{prot} ($M^{-1}\cdot s^{-1}$)	k_{deprot}/k_{prot}	pK_a (Schiff base)
octanoate	4.89	590	152	3.88	4.30 ± 0.06
acetate	4.75	42			
azide	4.72	8075	3900	2.07	4.41 ± 0.06
formate	3.75	585	2180	0.27	4.32 ± 0.03
cyanate	3.66	2530	8690	0.29	4.17 ± 0.06
fluoride	3.17	120	2750	0.044	4.50 ± 0.15

[a] The values in this table were calculated from experiments with different concentrations of catalysts, such as described in Figure 3 for azide, using the kinetic model in Figure 2 and eq 5 and 6. The averages and standard deviations in the last column are from three to four determinations.

and reverse reactions in (3), pK_a is the acid dissociation constant in (4), and [base] is the total concentration of the base. Because the pH in these experiments was well above the pK_a of the bases, $[B^-]$ is essentially equal to [base]. The two rate constants calculated in this way are shown in Table I for a variety of bases, arranged in the order of their pK_a. It is seen in Table I that a large number of anionic bases catalyze the de- and reprotonation and to different extents. Uncouplers of oxidative phosphorylation, such as dinitrophenol or SF 6847, were ineffective as proton acceptors (not shown). There are only a few nonionic bases in the same pK_a range; one of these, pyridine (pK_a = 5.25), was found to be completely without effect on the deprotonation (not shown).

The data obtained allowed also the estimation of the pK_a for the deprotonation of the retinal Schiff base, because this $pK_a = -\log k_4/k_5$. As seen in Table I, the observed pK_a for the Schiff base is essentially constant and near 4.3 in the reactions catalyzed by bases with a pK_a that varies between 3.2 and 4.9. Analysis of steady-state and flash deprotonation data was reported (Oesterhelt et al., 1985) to yield a pK_a of 4.8 in 1 M NaCl buffer.

Deprotonation of Halorhodopsin in Cell Envelope Vesicles. The conversion of halorhodopsin into HR_{410}^L can be followed also in the envelope vesicles, by measuring time-dependent inactivation of transport during illumination in the presence of azide or other bases (Hegemann et al., 1985b). In these measurements the pigment is examined in its membrane-bound form, rather than in detergent micelles, as in the experiments described above. One of the objectives of this line of investigation was to explore the topology of the proton release. Vesicles were illuminated, with the exterior medium well buffered at pH 8.0. Since the vesicles take up large quantities of protons during illumination in response to the inside negative membrane potential (MacDonald et al., 1979; Greene & Lanyi, 1979), the inside pH is lowered significantly. If buffering is provided inside the vesicles, however, the pH inside will remain near 8.0. If the proton release upon the $HR_{578}\cdot Cl^- \rightarrow HR_{410}^L$ reaction is from the exterior membrane surface, this should have no effect on the rate of halorhodopsin inactivation. If, on the other hand, the proton release is from the interior surface, buffering on the inside will cause increased inactivation of the transport relative to the rate with internally unbuffered vesicles. Figure 4 shows results with cell envelope vesicles osmotically shocked to load them either with unbuffered saline (A and B) or with well-buffered saline (C and D). The development of membrane potential was followed by measuring TPP^+ uptake with an electrode. Controls for the azide additions (B and D) were provided by adding NaCl instead (A and C). It is evident from Figure 4 that buffering the interior of the vesicles increased the rate of azide-dependent inactivation by about 3-fold, after correcting for the controls.

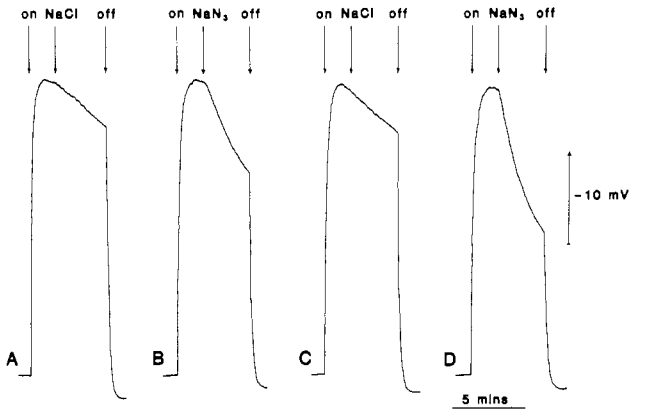

FIGURE 4: Inactivation of halorhodopsin by illumination of cell envelope vesicles in the presence of azide. The vesicles were osmotically shocked to load them with either unbuffered NaCl, followed by addition of EPPS, pH 8.0, to 100 mM final concentration (A and B), or with NaCl plus 100 mM EPPS, pH 8.0 (C and D), as described under Materials and Methods. The traces are recordings with a TPP^+ electrode and measure the creation of membrane potential across the vesicle membranes. The beginning and end of the illumination is indicated by arrows labeled "on" and "off". Additions were either NaN_3, to a final concentration of 2 mM, or the equivalent amount of NaCl as control. Vertical scale refers to the signal from the TPP^+ electrode; the maximum membrane potential achieved across the vesicle membranes is estimated to be about −170 mV.

This result is consistent with proton release from halorhodopsin on the interior surface of the vesicle membrane.

Another question is which side the azide binds to halorhodopsin. If the azide were to bind on the membrane side facing the interior of the vesicle, adding the azide during the illumination should result in slower halorhodopsin inactivation than after adding it in the dark, because the membrane potential (negative inside) present under these conditions will tend to exclude the azide from the vesicles. This was indeed found to be the case: the inactivation of transport was several times more rapid when the azide was added before the illumination was started (not shown).

In addition to azide, many of the other bases shown to deprotonate halorhodopsin in Table I were tested for inactivation of transport, in experiments similar to those in Figure 4. The rate of inactivation was a linear function of base concentration in all experiments (not shown). While the slope of this relationship is equivalent in principle to k_{deprot} calculated in Table I for each base, the absolute magnitude of k_{deprot} could not be estimated from these results without knowing the steady-state amount of HR_{640} produced during the illumination. Comparison of the rate constants calculated from the vesicle experiments (in arbitrary units) with those from the flash experiments shows, however, that the relative catalytic activities of the different bases agree well in the two systems (Figure 5). Thus, the specificity observed for the bases is not dependent on whether the halorhodopsin is in a detergent micelle or in the halobacterial membrane.

Discussion

The greatly lowered pK_a for the deprotonation of the halorhodopsin Schiff base after isomerization of the retinal in HR_{640} suggests that, as in bacteriorhodopsin, the Schiff-base nitrogen in this pigment moves to a less electronegative environment upon the configuration transition. However, while the protonation reactions of all-trans halorhodopsin are rapid and essentially diffusion controlled (Gutman & Nachliel, 1985), the deprotonation and reprotonation of its 13-cis photointermediate appear to be hindered by a kinetic barrier. This barrier is partially overcome by suitable bases, which

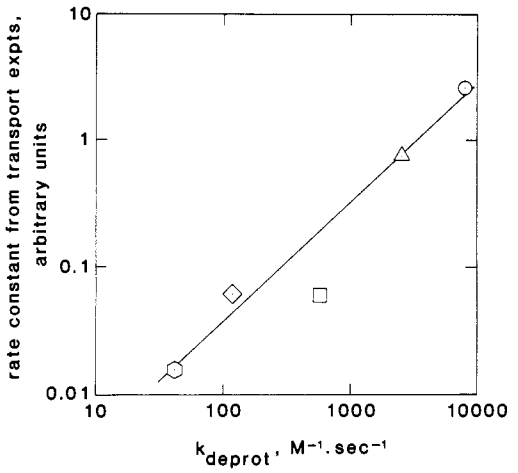

FIGURE 5: Comparison of relative rates of deprotonation from transport experiments with k_{deprot} values from spectroscopic experiments. The inactivation of halorhodopsin upon addition of various bases was measured in experiments such as shown in Figure 4. The rate of decrease in membrane potential was linearly dependent on the concentration of the bases (not shown); the slope of these lines are given on the ordinate. Calculated values of k_{deprot} from Table I are given on the abscissa. Symbols: (⊙), azide; (▲), cyanate; (⊡), formate; (◇), fluoride; (⊙), acetate.

catalyze the de- and reprotonation. The base-catalyzed protonation changes of the halorhodopsin Schiff base could be mediated by a binding site for the bases, at a suitable location in or on the protein along the proton conduction pathway. Earlier results with azide and cyanate (Oesterhelt et al., 1985) seemed to indicate that the catalytic effect saturated at moderate catalyst concentration, and the question could be raised as to which anion binding site, described already in this system (Schobert et al., 1986), was utilized by the anionic catalysts. It is evident from the present work, however, that the saturation effect is a fortuitous consequence of the competition between the $HR_{640} \rightarrow HR_{410}{}^{L}$ and $HR_{640} \rightarrow HR_{565}$ reactions (see Figure 2 for the kinetic model and Figure 3 for the prediction of the model). The dependency of the rate constant of the former reaction, k_4, on azide concentration (Figure 3) reveals that, in fact, the azide binds with very low apparent affinity, i.e., with an apparent K_D well above 100 mM. This is true for the large variety of bases tested for their effect on deprotonation (not shown), even though the absolute rates of the deprotonation were highly dependent on the nature of the base (Table I). The concentration dependency of the catalytic effect is therefore better described by a simple partitioning of the bases between the aqueous phase and the protein interior, where the Schiff base is likely to be located. This kind of mechanism would show low apparent affinity and lack of saturation, as found, but a distinct selectivity based on hydrophobicity and molecular size. The evidence with vesicles (Figure 4 and experiments described in the text) suggests that azide binding and proton release both occur inside the vesicle, i.e., on the face of the membrane where chloride is released during transport. These findings indicate that proton conduction between the protein interior and the aqueous medium in this system is somewhat similar to uncoupling of oxidative phosphorylation (although, as mentioned, classical uncouplers do not function here) but better described as "decoupling", defined by Rottenberg (1983) as proton shuttling by extrinsic agents between the interior and the exterior of a membrane. This is an important difference between halorhodopsin and bacteriorhodopsin, since in the latter the protein is thought to supply residues for the effective conduction of protons to and from the Schiff base (Engelhard et al., 1985).

Known anion binding sites in halorhodopsin do not seem to be the loci for the azide-catalyzed protonation changes: azide cannot act as proton acceptor when bound to site I, because this is a surface site with a K_D of about 10 mM for this anion (Schobert et al., 1986; Schobert & Lanyi, 1986), and site II cannot be the location where azide is protonated either, because it binds chloride, bromide, and iodide only (Steiner et al., 1984; Hazemoto et al., 1985).

A mechanism based on a partitioning equilibrium for the bases between the medium and the protein interior predicts that the catalytic activity of various bases will depend only on their pK_a; i.e., bases with high pK_a will be better proton acceptors but poorer proton donors and vice versa. This was found to be the case: the data in Table I show that the pK_a of the base is a good predictor of the k_{deprot}/k_{prot} ratio.

Whenever the deprotonation experiments were carried out in the absence of chloride, the photointermediate that would deprotonate was, naturally, assumed to be HR_{640}. In the presence of chloride $HR_{520}{\cdot}Cl^-$ is also produced (Oesterhelt et al., 1985; Lanyi & Vodyanoy, 1986), and the question may be asked whether this intermediate will deprotonate. Results from Oesterhelt et al. (1985) suggest that only HR_{640} can deprotonate, because the chloride dependency of the steady-state accumulation of $HR_{410}{}^{L}$ agreed with that of HR_{640} rather than with that of the sum of the two photointermediates; i.e., it was found to be chloride independent. The inability of $HR_{520}{\cdot}Cl^-$ to lose a proton, even in the presence of azide, may originate from either unfavorable geometry for proton transfer in this species or an elevated Schiff-base pK_a. In either case, it appears that the deprotonation of the Schiff base of halorhodopsin is very sensitive to changing environmental influences inside the protein, which must accompany the primary photoreaction and the subsequent events in the photocycle.

ACKNOWLEDGMENTS

I am very grateful to Kitiman Greethong for experimental assistance and to Drs. D. Oesterhelt, P. Hegemann, J. Tittor, and M. Gutman for critical comments.

REFERENCES

Alshuth, T., Stockburger, M., Hegemann, P., & Oesterhelt, D. (1985) *FEBS Lett. 179*, 55–59.

Bamberg, E., Hegemann, P., & Oesterhelt, D. (1984) *Biochim. Biophys. Acta 773*, 53–60.

Engelhard, M., Gerwert, K., Hess, B., Kreutz, W., & Siebert, F. (1985) *Biochemistry 24*, 400–407.

Greene, R. V., & Lanyi, J. K. (1979) *J. Biol. Chem. 254*, 10986–10994.

Gutman, M., & Nachliel, E. (1985) *FEBS Lett. 190*, 29–32.

Hazemoto, N., Kamo, N., Kobatake, Y., Tsuda, M., & Terayama, Y. (1984) *Biophys. J. 45*, 1073–1077.

Hegemann, P., Oesterhelt, D., & Steiner, M. (1985a) *EMBO J. 4*, 2347–2350.

Hegemann, P., Oesterhelt, D., & Bamberg, E. (1985b) *Biochim. Biophys. Acta 819*, 195–205.

Kamo, N., Racanelli, T., & Packer, L. (1982) *Methods Enzymol. 88*, 356–360.

Lanyi, J. K. (1984a) *FEBS Lett. 175*, 337–342.

Lanyi, J. K. (1984b) in *Comparative Biochemistry: Bioenergetics* (Ernster, L., Ed.) pp 315–350, Elsevier, Amsterdam.

Lanyi, J. K., & MacDonald, R. E. (1979) *Methods Enzymol. 56*, 398–407.

Lanyi, J. K., & Schobert, B. (1983) *Biochemistry 22*, 2763–2769.

Lanyi, J. K., & Vodyanoy, V. (1986) *Biochemistry 25*, 1465–1470.

Lewis, A., Spoonhower, J., Bogomolni, R. A., Lozier, R. H., & Stoeckenius, W. (1974) *Proc. Natl. Acad. Sci. U.S.A. 71*, 4462–4466.
MacDonald R. E., Greene, R. V., Clark, R. D., & Lindley, E. V. (1979) *J. Biol. Chem. 254*, 11831–11838.
Maeda, A., Ogurusu, T., Yoshizawa, T., & Kitagawa, T. (1985) *Biochemistry 24*, 2517–2521.
Oesterhelt, D., Hegemann, P., & Tittor, J. (1985) *EMBO J. 4*, 2351–2356.
Ogurusu, T., Maeda, A., Sasaki, N., & Yoshizawa, T. (1982) *Biochim. Biophys. Acta 682*, 446–451.
Ogurusu, T., Maeda, A., & Yoshizawa, T. (1984) *J. Biochem. (Tokyo) 95*, 1073–1082.
Polland, H.-J., Franz, M. A., Zinth, W., Kaiser, W., Hegemann, P., & Oesterhelt, D. (1985) *Biophys. J. 47*, 55–59.
Rottenberg, H. (1983) *Proc. Natl. Acad. Sci. U.S.A. 80*, 3313–3317.
Schobert, B., & Lanyi, J. K. (1982) *J. Biol. Chem. 257*, 10306–10313.
Schobert, B., & Lanyi, J. K. (1986) *Biochemistry 25*, 4163–4167.
Schobert, B., Lanyi, J. K., & Cragoe, E. J., Jr. (1983) *J. Biol. Chem. 258*, 15158–15164.
Schobert, B., Lanyi, J. K., & Oesterhelt, D. (1986) *J. Biol. Chem. 261*, 2690–2696.
Smith, S. O., Marvin, M. J., Bogomolni, R. A., & Mathies, R. A. (1984) *J. Biol. Chem. 259*, 12326–12329.
Steiner, M., & Oesterhelt, D. (1983) *EMBO J. 2*, 1379–1384.
Steiner, M., Oesterhelt, D., Ariki, M., & Lanyi, J. K. (1984) *J. Biol. Chem. 259*, 2179–2184.
Stoeckenius, W., & Bogomolni R. A. (1982) *Annu. Rev. Biochem. 52*, 587–616.
Stoeckenius, W., Lozier, R. H., Bogomolni, R. A. (1979) *Biochim. Biophys. Acta 505*, 215–278.

Immunochemical Detection of Guanine Nucleotide Binding Proteins Mono-ADP-ribosylated by Bacterial Toxins

B. Eide,[‡] P. Gierschik,[§] and A. Spiegel*

Howard Hughes Medical Institute and Molecular Pathophysiology Section, National Institute of Arthritis, Diabetes, and Digestive and Kidney Diseases, National Institutes of Health, Bethesda, Maryland 20892

Received May 9, 1986

ABSTRACT: Rabbits immunized with ADP-ribose chemically conjugated to carrier proteins developed antibodies reactive against guanine nucleotide binding proteins (G proteins) that had been mono-ADP-ribosylated by bacterial toxins. Antibody reactivity on immunoblots was strictly dependent on incubation of substrate proteins with both toxin and NAD and was quantitatively related to the extent of ADP-ribosylation. G_i, G_o, and transducin (ADP-ribosylated by pertussis toxin) and elongation factor II (EF-II) (ADP-ribosylated by pseudomonas exotoxin) all reacted with ADP-ribose antibodies. ADP-ribose antibodies detected the ADP-ribosylation of an approximately 40-kilodalton (kDa) membrane protein related to G_i in intact human neutrophils incubated with pertussis toxin and the ADP-ribosylation of an approximately 90-kDa cytosolic protein, presumably EF-II, in intact HUT-102 cells incubated with pseudomonas exotoxin. ADP-ribose antibodies represent a novel tool for the identification and study of G proteins and other substrates for bacterial toxin ADP-ribosylation.

Mono-ADP-ribosylation is a posttranslational modification in which the ADP-ribose moiety of NAD is covalently linked to one of a defined group of protein substrates (Ueda & Hayaishi, 1985). Mono-ADP-ribosylation of protein substrates from eukaryotic cells may be catalyzed either in whole cells or in broken cell preparations by a variety of microbial toxins (Honjo et al., 1968; Iglewski & Kabat, 1975; Cassel & Pfeuffer, 1978; Gill & Meren, 1978; Moss & Richardson, 1978; Katada & Ui, 1982) or endogenous enzymes (Moss & Vaughan, 1978; Moss & Stanley, 1981; DeWolf et al., 1981; Richter et al., 1983; Tanigawa et al., 1984; Lee & Iglewski, 1984). These reactions have been monitored in broken cell preparations by using radioactively labeled NAD. In toxin-treated intact cells, only indirect assays which measure either functional effects or the extinction of toxin substrate availability have been used. We sought an alternative method which would permit direct detection of mono-ADP-ribosylation of substrates, even in whole cells treated with bacterial toxins. We therefore immunized rabbits with ADP-ribose chemically conjugated to bovine serum albumin (BSA)[1] in an attempt to obtain antibodies capable of recognizing ADP-ribosylated proteins.

Materials and Methods

Materials. EF-II, pseudomonas exotoxin, rabbit reticulocyte lysate, and HUT-102 cells were generously provided by Dr. D. Fitzgerald (NCI). Pertussis toxin was contributed by Dr. R. Sekura (NICHD). Glutamine synthetase was the gift of Dr. S. G. Rhee (NHLBI). Sources of other materials used in protein determination, SDS gel electrophoresis, toxin-cat-

* Correspondence should be addressed to this author.
‡ HHMI/NIH Medical Scholars Program.
§ Present address: Department of Pharmacology, University of Heidelberg, West Germany.

[1] Abbreviations: ADPR, ADP-ribose; KLH, keyhole limpet hemocyanin; BSA, bovine serum albumin; G proteins, guanine nucleotide binding regulatory proteins; G_i, inhibitory G protein associated with adenylate cyclase; G_o, guanine nucleotide binding protein isolated from bovine brain; EF-II, elongation factor II; kDa, kilodalton(s); ELISA, enzyme-linked immunosorbant assay; SDS, sodium dodecyl sulfate; Tris-HCl, tris(hydroxymethyl)aminomethane hydrochloride; DTT, dithiothreitol; EDTA, ethylenediaminetetraacetic acid.